

ENERGETIC NEUTRONS, PROTONS, AND GAMMA RAYS DURING THE 1990 MAY 24 SOLAR COSMIC-RAY EVENT

H. DEBRUNNER,¹ J. A. LOCKWOOD,² C. BARAT,³ R. BÜTIKOFER,¹ J. P. DEZALAY,³ E. FLÜCKIGER,¹
A. KUZNETSOV,⁴ J. M. RYAN,² R. SUNYAEV,⁴ O. V. TEREKHOV,⁴ G. TROTET,⁵ AND N. VILMER⁵

Received 1995 December 26; accepted 1996 November 4

ABSTRACT

The solar cosmic-ray event on 1990 May 24 can be divided into three phases: a first impulsive production of γ -rays and greater than 200 MeV neutrons; a second slower phase during which there were high-energy protons at the Sun for ~ 20 minutes producing pions and high-energy neutrons; and a third phase when the protons observed by the *IMP 8* and *GOES* spacecraft and by neutron monitors were injected into interplanetary space. This third phase started after the onset of the event but before the second phase had ceased. We found that high-energy neutron production occurred during the last 60 s of the impulsive phase and at least the first 19 minutes of the second phase. During the second phase the high energy-neutron and γ -ray emissions decayed more slowly than either the 2.2 MeV or 4–7 MeV γ -ray line emissions. A two-component neutron energy spectrum that changes between the first and second phases gives a reasonable fit to the count rate increase recorded by the Climax neutron monitor. From the fit we infer that the integrated neutron emissivity at the Sun was $\sim 3.5 \times 10^{30} \text{ sr}^{-1}$ for $E > 100 \text{ MeV}$. The maximum intensity of $P > 1.5 \text{ GV}$ solar protons near the Earth was $4.5 \times 10^3 (\text{m}^2 \text{ sr s})^{-1}$. The differential solar proton energy flux (dJ/dE) as a function of rigidity at the Sun can be described by an evolving power-law spectrum. We estimate that the number of escaping protons with $E > 30 \text{ MeV}$ in the third phase was 7%–14% of the number of protons required to produce the solar neutron increase at the Earth. Although it is attractive to assume that the interplanetary solar protons simply leaked out from the trapping region at the Sun, the data suggest that the interplanetary solar protons were not from the population of energetic particles that produced the neutron and γ -ray emissions but were freshly accelerated during the third phase of the solar flare.

Subject headings: cosmic rays — elementary particles — gamma rays: observations — Sun: flares — Sun: particle emission

1. INTRODUCTION

The solar cosmic-ray event observed on 1990 May 24 with ground-level neutron monitors (NMs) and spacecraft experiments was associated with the solar flare at 2046 UT in NOAA region 6063 located at N36°W76° (heliocentric angle = 80°). There were two accompanying large NM count rate increases. The first increase that started at 2049 UT was due to direct solar neutrons as first suggested by Shea, Smart, & Pyle (1991). This increase was of relatively short duration (~ 25 minutes) and was observed only by NMs in North America (Fig. 1). It was the largest solar neutron increase ever recorded by NMs. The second increase began at 2102:30 \pm 00:30 UT and was produced by energetic solar protons. It had a duration of more than 6 hr and was highly anisotropic at relativistic energies for more than 1 hr.

Kocharov et al. (1994) analyzed the H α , microwave, γ -ray, and neutron emissions during the first NM count rate increase and deduced the neutron injection-time profile and energy spectrum. Terekhov et al. (1993) estimated the 2.2 MeV γ -ray line emission using data from the PHEBUS

instrument on the *Granat* spacecraft. They also deduced an intensity-time profile of the neutron emission for energies greater than 120 MeV. Debrunner, Lockwood, & Ryan (1993), in a previous analysis of this event, estimated the integrated neutron flux at the Earth to be 2.5×10^4 neutrons cm^{-2} for $E \geq 100 \text{ MeV}$, i.e., about an order of magnitude greater than that estimated by Kocharov et al. (1994).

For the second NM increase on 1990 May 24 Debrunner et al. (1993) found that the high-energy solar protons near $\sim 2120 \text{ UT}$ had a differential rigidity spectrum proportional to $P^{-5.5}$. They also concluded that these solar protons were accelerated by a coronal shock and that the total number of protons with $P > 0.25 \text{ GV}$ ($E_p \geq 30 \text{ MeV}$) emitted at the Sun was less than 2×10^{34} . This is less than 10% of the total number of protons ($E_p \geq 30 \text{ MeV}$) required at the Sun to produce the solar neutron fluence measured at the Earth during the first increase.

In this analysis we divide the event into three phases (see Table 1): (i) an impulsive phase from 2047:50 to 2049:24 UT during which neutrons and γ -rays were produced; (ii) a second slower phase lasting from 2049:24 to $\sim 2109 \text{ UT}$ with neutron and predominantly high-energy γ -ray emissions; and (iii) a third phase from ~ 2052 to at least 2200 UT when solar protons were injected into interplanetary space near the Sun. To estimate the neutron emissivity at the Sun we use the γ -ray measurements by the PHEBUS detector on the *Granat* spacecraft. We evaluate the intensity-time profile of the pion-production at the Sun and assume that the greater than 200 MeV neutron production follows the intensity-time profile of the pion-related γ -rays. We also determine the onset time of the proton event at the

¹ Physikalisches Institut, University of Bern, 3012 Bern, Switzerland.

² Space Science Center, University of New Hampshire, Durham, NH 03842.

³ Centre d'Etude Spatiale des Rayonnements, CNRS/UPS, BP4346, 31029 Toulouse, France.

⁴ Space Research Institute, Profsoyuznaya 84/32, 117810 Moscow, Russia.

⁵ Observatoire de Paris, Section de Meudon, DASOP and CNRS/URA1756, 92195 Meudon, France.

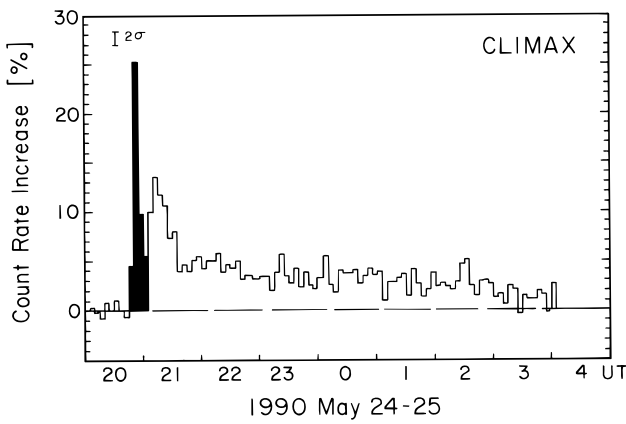


FIG. 1a

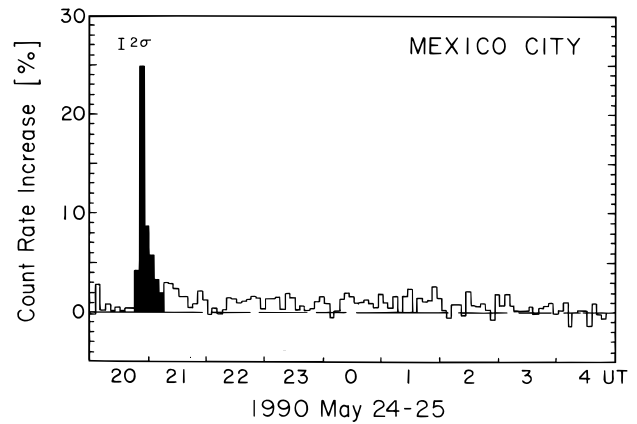


FIG. 1b

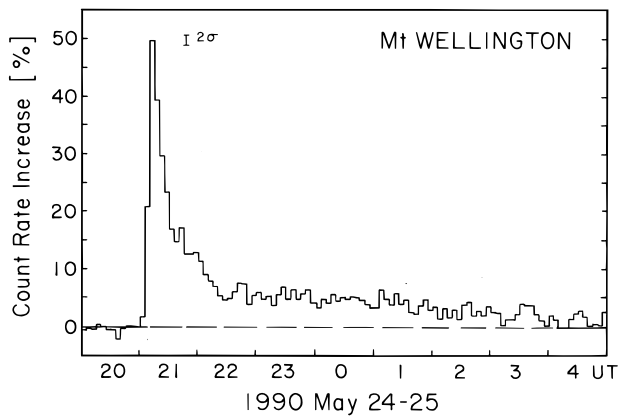


FIG. 1c

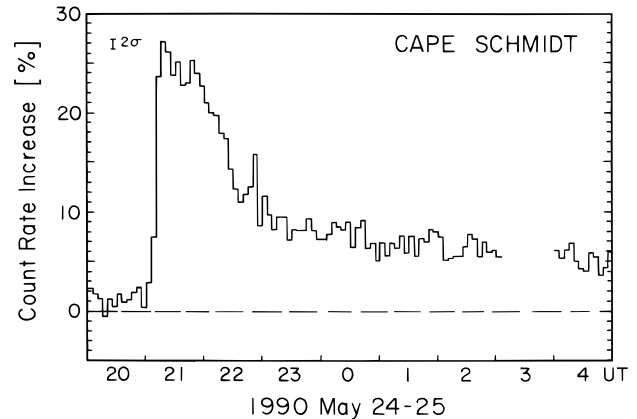


FIG. 1d

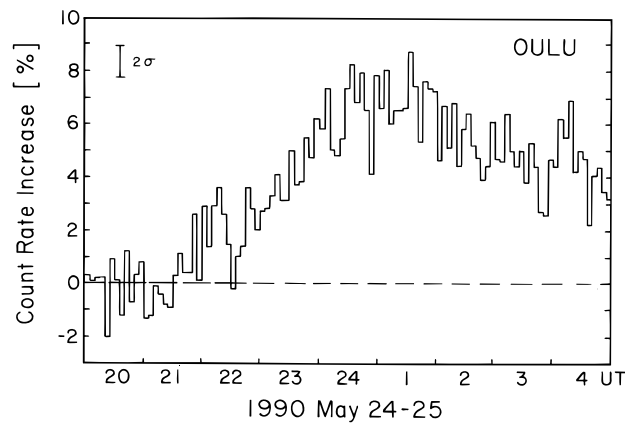


FIG. 1e

FIG. 1.—5-minute average count rate increases of some NMs from 2000 UT on 1990 May 24 to 0500 UT on May 25. The increases in the dark areas of (a) and (b) were due to solar neutrons.

Earth as a function of energy, as well as the energy spectrum of the solar protons from about 50 to 5000 MeV near the Earth. For the anisotropic phase we then extrapolate these spectra back to the Sun to determine the source proton energy spectra. Finally, we discuss the relationship between the protons producing the γ -rays and neutrons at the Sun and the interplanetary protons.

2. GAMMA-RAY MEASUREMENTS

The PHEBUS instrument on the *Granat* spacecraft consists of six detectors with axes parallel to the Cartesian coordinate system of GRANAT (Barat et al. 1988). Each

detector is a cylindrical BGO scintillator with a diameter of 7.8 cm and a length of 12 cm surrounded by a plastic anti-coincidence shield. In this study we have used the γ -ray data from the two detectors on the +X and -Y axes (essentially perpendicular to the Earth-Sun line). The nominal energy range from 100 keV to 100 MeV is covered by 42 channels with a time resolution of 1 s at $E < 10$ MeV and 4 s at $E > 10$ MeV.

Figure 2a displays the 4 s average γ -ray count rates from the -Y detector in the 10–24 MeV and 60–95 MeV energy bands from ~ 2047 to ~ 2057 UT. Figure 2b shows the expanded rates in the 10–24 MeV, 60–75 MeV, and 75–95

TABLE 1
TIME SEQUENCE OF THE 1990 MAY 24 SOLAR COSMIC-RAY EVENT

Event	Time
Onset of the γ -ray event ^a	2047:50 UT
Estimated start of the Moreton wave (Kocharov et al. 1994)	> 2047:40 UT
First peak of the 75–95 MeV γ -ray emission	2048:12 UT
Onset of the high energy neutron production at the Sun	2048:18 UT
Maximum intensity of the 2.2 MeV and 4–7 MeV γ -ray line emissions	2048:28 UT
Second peak of the 75–95 MeV γ -ray emission	2048:36 UT
Beginning of the gradual phase of the 60–95 MeV γ -ray emission	2049:24 UT
Onset of the emission of the first interplanetary protons at low energies	2052 \pm 2 UT
Onset of the emission of the first interplanetary protons at NM energies	2054 \pm 2 UT
Estimated end of the high energy neutron production at the Sun	2109:30 UT

^a At the 3σ level for the > 60 MeV γ -ray count rates.

MeV energy bands during the impulsive phase from 2047:45 to 2049:15 UT. The onset times of the emissions in the 60–75 MeV and 75–95 MeV bands, defined as the times when the count rate increase is 3σ above the background, were $2047:48 \pm 00:02$ UT and $2047:52 \pm 00:02$ UT, respectively. We thus take $2047:50 \pm 00:04$ UT as the start of the greater than 60 MeV γ -ray event. There were two maxima in the 60–75 MeV and 75–95 MeV count rates at $2048:12 \pm 00:04$ and $2048:36 \pm 00:04$ UT, respectively. After the second maximum the count rates decreased rapidly for about 50 s and then decayed slowly over the next 8 minutes with the exception of a bump observed between 2050 and 2052 UT. The 60–95 MeV count rates were still greater than the background 9 minutes after the second peak. At this time the data transmission stopped due to the limited on-board memory.

Talon et al. (1993) noted that the two peaks in the 60–75 MeV channel during the impulsive phase have comparable intensities (Fig. 2*b*) whereas in the 75–95 MeV channel the intensity of the second peak was about twice that of the first. This indicates that there were relatively more greater than 75 MeV γ -rays present in the second peak than in the first peak. Figure 3 shows the count rate spectra measured above 10 MeV during the rise and decay of the first (panels *a* and *b*) peak and during the rise and decay of the second peak (panels *c* and *d*). Power-law photon spectra were then

folded into the instrumental response of the PHEBUS detector and fitted to the measured spectra from 10 to 48 MeV during the two peaks. These are shown as continuous lines in Figure 3. The slope of the resulting power-law photon spectra remains approximately constant during the two peaks with a spectral index of 2.2 ± 0.1 . The photon spectra are then extrapolated to 100 MeV for comparison with the measured spectra above 50 MeV. The observed spectrum in Figure 3 steepens above 50 MeV during the first peak while during the second peak there is a clear excess of photons when compared with the extrapolated power-law photon spectrum. Figure 4 shows the ratio of the 60–95 MeV to the 10–24 MeV count rates starting at 2048:22 UT, in the valley between the two peaks in the impulsive phase. We see that the ratio increases rapidly to the time of the second peak, then increases steadily until ~ 2052 UT, after which it remains relatively constant until 2057 UT. From Figures 3 and 4 we conclude that: (i) the greater than 10 MeV γ -ray emission during the first peak was produced primarily by relativistic electrons; (ii) the greater than 50 MeV γ -ray emission during the second peak was dominated by neutral pion decay radiation; and (iii) the pion-related γ -rays also contributed to the emission during the second phase (Fig. 4).

In Figures 2*a* and 5 there is a bump in the high-energy count rates from 2050 to 2052 UT that coincides with the

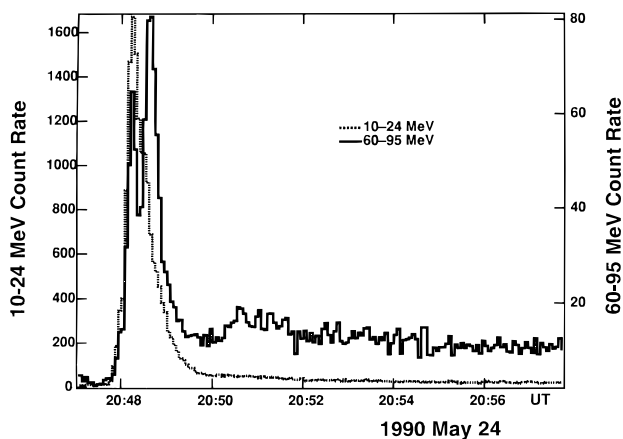


FIG. 2*a*

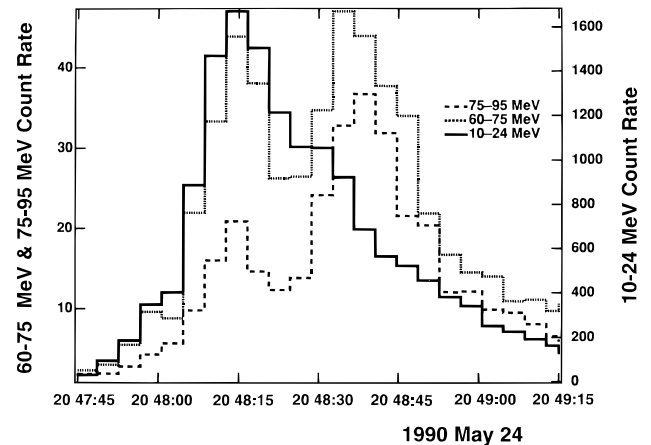


FIG. 2*b*

FIG. 2.—(a) Count rates (cps) of the 60–95 MeV and 10–24 MeV γ -rays measured by the PHEBUS detector on the *Granat* spacecraft from 20:47 to 20:58 UT on 1990 May 24. The count rate of 1 count s^{-1} corresponds to photon fluxes of $\sim 2.7 \times 10^{-2}$ and 5×10^{-2} photons $\text{cm}^{-2} \text{ s}^{-1}$ in 10–24 MeV and the 60–95 MeV bands, respectively. (b) Count rates (cps) in the 10–24 MeV, 60–75 MeV, and 75–95 MeV energy bands of the PHEBUS detector during the impulsive phase of the 1990 May 24 solar cosmic-ray event. The count rate of 1 count s^{-1} corresponds to photon fluxes of $\sim 2.7 \times 10^{-2}$, 4.3×10^{-2} , and 5.6×10^{-2} photons $\text{cm}^{-2} \text{ s}^{-1}$ in the 10–24 MeV, 60–75 MeV, and 75–95 MeV bands, respectively.

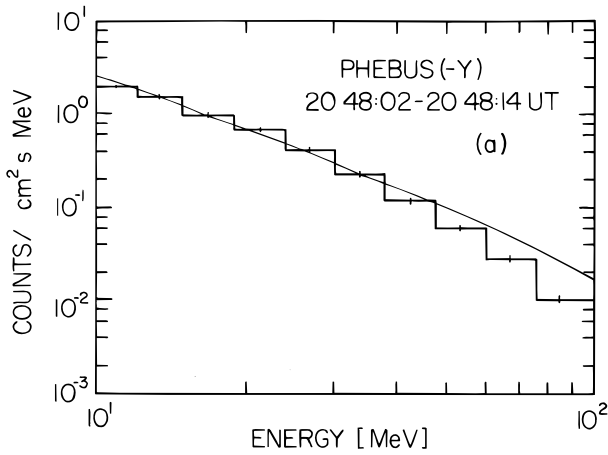


FIG. 3a

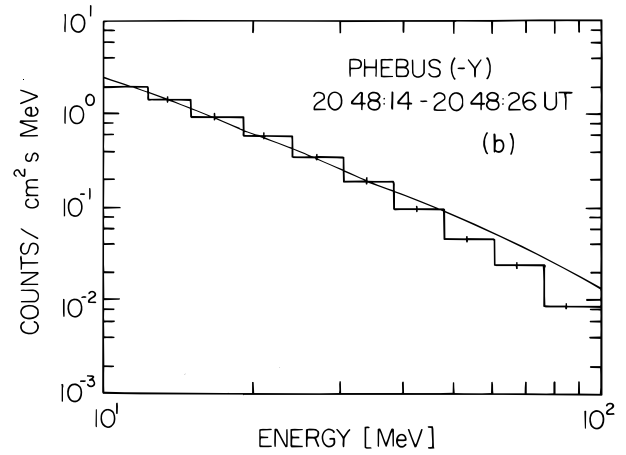


FIG. 3b

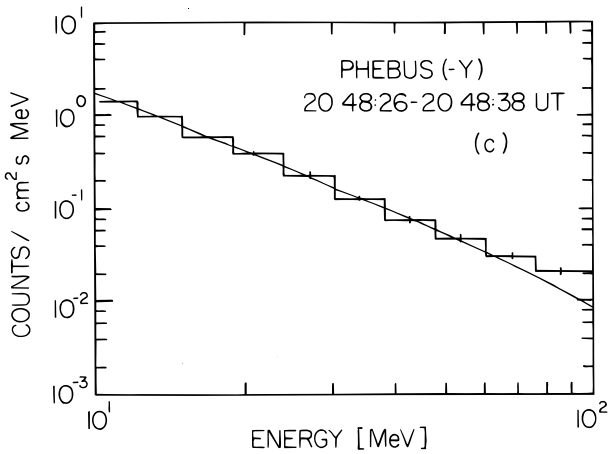


FIG. 3c

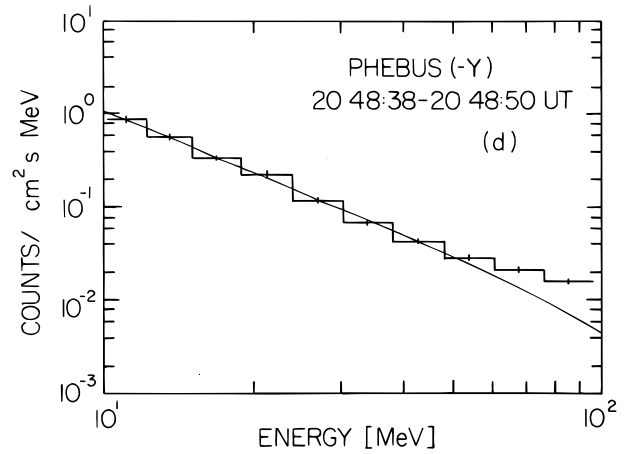


FIG. 3d

FIG. 3.—(a) Observed count rate spectrum from 10 to 100 MeV with error bars and a power-law photon spectrum convolved with the PHEBUS instrumental response, giving the best fit to the 10–48 MeV count rate spectrum, and then extrapolated to 100 MeV for 2048:02–2048:14 UT on 1990 May 24. (b) Same as (a) for 2048:14–2048:26 UT. (c) Same as (a) for 2048:26–2048:38 UT. (d) Same as (a) for 2048:38–2048:50 UT.

maximum count rate of the Climax NM due to solar neutrons (Fig. 1a). It suggests that the PHEBUS response in these channels might have been influenced by the intense flux of solar neutrons (Terekhov et al. 1993; Talon et al. 1993). It is thus important to estimate the effect of neutrons on the pion production profile shown in Figure 5 since this

profile will be used as the intensity-time profile of the neutron production.

As we do not know the exact response of the PHEBUS BGO γ -ray instrument to neutrons, we used two different methods to estimate the contribution of neutrons to the pion production profile in the second phase. First, we calcu-

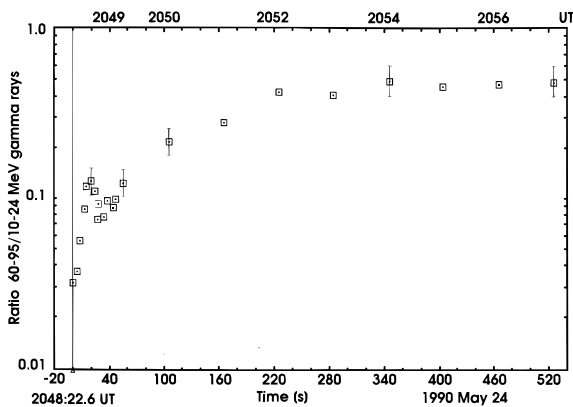


FIG. 4.—Ratio of the 60–95 MeV to 10–24 MeV count rates of the PHEBUS detector starting at 2048:22 UT on 1990 May 24.

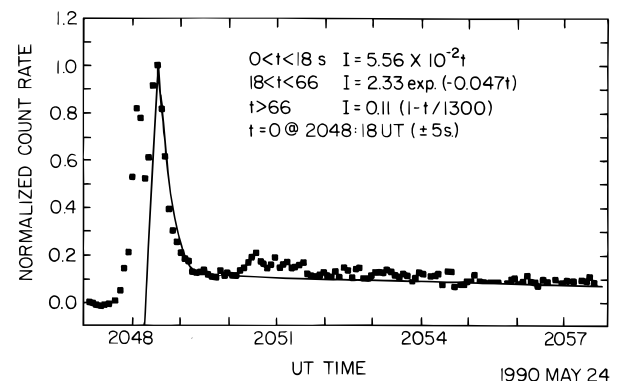


FIG. 5.—Normalized 60–95 MeV 5 s average count rate from 2047 to 2058 UT on 1990 May 24 and the pion production profile deduced from the data of the PHEBUS detector (heavy line).

lated the solar neutron flux at Earth as a function of energy and time, assuming that the intensity-time profile of the pion-related γ -rays indicated by the heavy line in Figure 5 represents the neutron production-time profile and does not include any neutron contribution. The results, presented in Appendix A, indicate that PHEBUS responds primarily to $E > 500$ MeV neutrons with an efficiency of 1%–2%. The estimated maximum excess count rate of the bump (2 counts s^{-1}) in the 75–95 MeV range due to greater than 500 MeV neutrons agreed with the observed excess rate from 2050 to 2052 UT. There appears to be little contribution to the count rate in the tail from 2050 to 2057 UT from the lower energy solar neutrons. Our second estimate of the contamination of the 75–95 MeV channel from solar neutrons starts with the assumption that all the counts in this energy window after 2053 UT were due to neutrons and that the PHEBUS detector efficiency for energetic neutron detection is not a strong function of energy. By analyzing the ≤ 75 MeV energy channels (Appendix A) we find that $\leq 30\%$ of the count rate in the 75–95 MeV channel was due to neutrons after 2053 UT. From these two different approaches we conclude that the decay constant for the pion-related γ -ray emission during the second phase was 900–1400 s. These two approaches are discussed in detail in Appendix A.

We then used the pion production curve shown as the heavy line in Figure 5 to represent the intensity-time profile of the high-energy neutron production. The bulk of the production of pion-related γ -rays, and hence of high-energy neutrons, started at 2048:18 UT (within the second high-energy spike in the impulsive phase), and rose rapidly to a maximum at 2048:36 UT. The production then decayed exponentially with an e -folding time of about 20 s. This phase was followed by a prolonged emission of pion-related γ -rays with a decay constant of 1300 s as indicated in Figure 5. We identify this prolonged emission as a second phase of the flare distinct from the impulsive phase.

In Figure 6 we have plotted the net 2.2 MeV and the 3.7–7.7 MeV (prompt nuclear line emission, nominally 4–7 MeV) excess count rates measured by the +X and –Y detectors from 2047–2057 UT corrected for dead time and energy scale nonlinearities. The 2.2 MeV γ -ray line emission in Figure 6 differs from that of Terekhov et al. (1993) because the plot given by these authors did not make these corrections. The 1990 May 24 event was one of the most intense solar flares detected by PHEBUS and instrumental effects, such as dead time and energy scale nonlinearities, complicated the analysis. To obtain the line emission excess we subtract from the total spectrum a power-law continuum determined by fitting the count rates between the 0.85–1.6 MeV and 8.7–15 MeV channels. Taking into account the instrumental parameters, the integrated total fluences are then ~ 1000 and ~ 960 photons cm^{-2} at 2.2 MeV and for the 3.7–7.7 MeV band, respectively. The 2.2 MeV to the 3.7–7.7 MeV fluence ratio is thus 1.0 ± 0.2 from 2048:24 UT (the start of the second high-energy γ -ray spike) until the last data at ~ 2057 UT. Using the calculations of Hua & Lingenfelter (1987) we estimate the spectral index of the power-law energy spectrum of the photons with $E < 500$ MeV to be 2.5–3.0 for this flare. As observed in other γ -ray line flares (Chupp et al. 1993; Trotter et al. 1994), the 3.7–7.7 MeV line emission started early in the event (20:47:32 UT). This indicates that, within statistical uncertainties, electrons and 10–100 MeV nucleon $^{-1}$ ions were accelerated simulta-

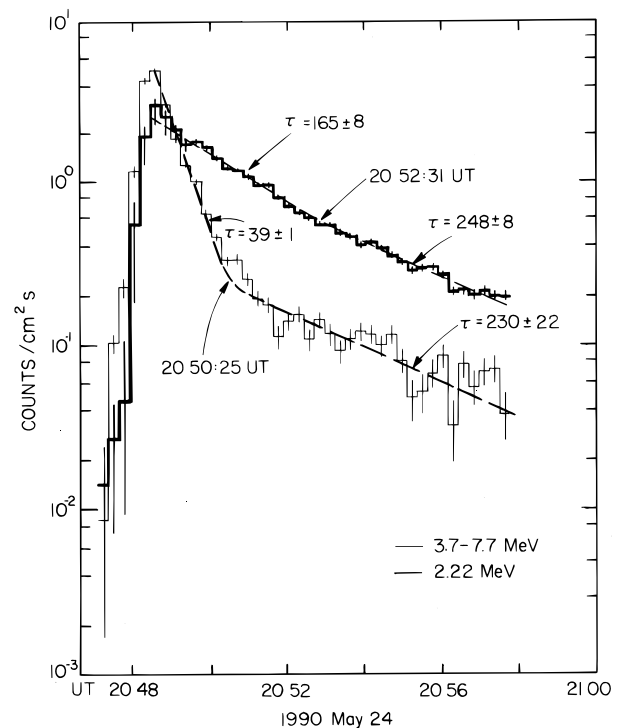


FIG. 6.—2.2 and 3.7–7.7 MeV γ -ray line intensities measured by the PHEBUS detector as a function of time during the 1990 May 24 solar flare event. For details see the text.

neously. The intensity maxima of the 2.2 MeV and 3.7–7.7 MeV fluxes occurred at 2048:28 UT, midway between the two spikes at higher energies. We therefore infer that the energy spectrum of the primary protons changed during the impulsive phase.

3. CALCULATION OF THE SOLAR NEUTRON FLUX

The increase in the counting rate of a neutron monitor due to solar neutrons can be written as

$$\Delta N_n(h, \theta, t) = \int \Phi_n(E_n, t) S_n(h, \theta, E_n) dE_n, \quad (1)$$

where ΔN_n is the absolute increase in the NM count rate due to solar neutrons (counts s^{-1}), Φ_n is the flux ($m^2 s MeV^{-1}$) of neutrons with energy E_n (MeV) incident at the top of the atmosphere at time t , S_n is the sensitive area of the NM (m^2) to primary neutrons, h ($g cm^{-2}$) is the depth of the NM in the atmosphere, and θ is the solar zenith angle (Debrunner, Flückiger, & Stein 1989). S_n for primary neutrons has been calculated by Debrunner et al. (1983, 1989, 1990) by a Monte Carlo nuclear cascade simulation and by Shibata (1994) using a different nuclear interaction model. In Appendix B we discuss the differences between the neutron response functions of Shibata (1994) and Debrunner et al. (1983, 1990). The Debrunner response function at $E > 200$ MeV is about twice as large as that of Shibata. At $E < 200$ MeV the two response functions diverge for reasons discussed in Appendix B. However, if the solar neutron production is prolonged, this difference in the response functions at low energies is not very significant.

In order to evaluate the neutron count rate ΔN_n of equation (1) in terms of the time-extended neutron pro-

duction at the Sun, we write

$$\Delta N_n(h, \theta, t) = R^{-2} \int_{t_{\min}}^{\infty} \mu(t - t_s) Q(E_n, t - t_s) dE_n / dt_s \times P(E_n) S_n(h, \theta, E_n) dt_s, \quad (2)$$

where R is the Earth-Sun distance, t_s is the difference between the Sun-Earth transit times for neutrons and photons, and $E_n(t_s)$ is the neutron energy as a function of t_s . The normalized intensity-time profile of the neutron emission is given by $\mu(t - t_s)$, where the time integral of μ is unity. The function Q is the directional neutron emissivity (neutrons $\text{sr}^{-1} \text{MeV}^{-1}$) and dE_n/dt_s is the neutron energy-time dispersion relation (Lingenfelter & Ramaty 1967). $P(E_n)$ is the probability for a neutron to reach the Earth before decay and S_n is the revised sensitive area of the Climax NM to primary neutrons (Fig. 16). The time t_{\min} corresponds to the upper cutoff of the neutron energy spectrum at the Sun.

We simulated the excess 1 minute count rates of the Climax NM during the first increase (Pyle 1991) using equation (2). It is evident that after 2105 UT the count rate at Climax (Fig. 1a) had begun to increase again due to the arrival of solar protons at the Earth. Therefore, we used the five-minute average rates from the 6NM64 monitor at Mexico City (Fig. 1b) to extend the observation time to 2115 UT. This extrapolation is valid because the count rate of the Mexico City NM decreased until 2115 UT (Fig. 1b). Only a small fraction of the NM count rate at Mexico City could have been due to solar protons in the time interval from 2110 to 2115 UT. This leads us to conclude that solar neutrons were still present in the count rates of the NMs at Climax and Mexico City until 2115 UT. The data of the Mexico City NM from 2105–2115 UT were corrected for the difference in atmospheric depth of Climax and Mexico City and the type of NM. This composite count rate profile for Climax was then compared with ΔN_n calculated with equation (2).

Debrunner et al. (1993) showed earlier that an impulsive neutron injection does not reproduce the count rate of the Climax NM during the 1990 May 24 solar flare increase. In that analysis they used the time profile of the 79–109 MeV γ -rays for the time-extended neutron injection, but did not separate the two peaks between 2048 and 2049 UT, and made a rough estimate of the contribution of solar neutrons to the 79–109 MeV γ -ray count rates as the neutron emissivity-time profile at the Sun, $\mu(t - t_s)$, and assuming $Q(E_n) \propto E_n^{-2.4}$ for $E_n > 100$ MeV with a high-energy cutoff at 4 GeV, Debrunner et al. (1993) obtained an adequate fit to the observed NM count rate increase at Climax. The spectral parameters were chosen because they have a good fit to the neutron observations of the 1982 June 3 solar neutron event (Chupp et al. 1987). This yielded a neutron fluence of $\sim 5 \times 10^{30}$ neutrons sr^{-1} above 100 MeV. However, it was necessary to assume that the emission of the first neutrons at the Sun was delayed by ~ 1.5 minutes with respect to the first 79–109 MeV γ -rays in order to have no neutron signal before 2049 UT.

In this analysis we use the intensity-time profile of the pion-related γ -rays shown in Figure 5 as the time profile of the high-energy neutron emission. We also use the γ -ray measurements to better interpret the neutron energy spectra. From Figures 2–4 and 6 we find that the energy

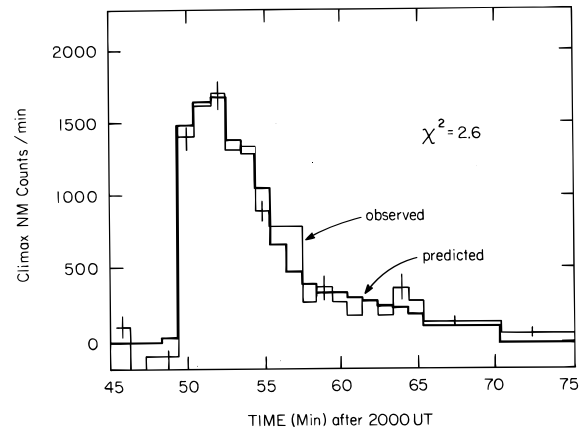


FIG. 7.—Comparison of the 1 minute average count rate increase at the Climax NM due to solar neutrons on 1990 May 24 with the predicted count rates for a time-extended neutron production at the Sun. Details are given in the text.

spectrum of the protons producing the γ -ray and neutron emissions varied from the second peak of the impulsive phase to the beginning of the second phase. Therefore, different energy spectra were taken for the neutron production during the impulsive and second phases. Thus, the present approach differs from our original analysis (Debrunner et al. 1993) in three respects: (1) the start of the neutron production is correlated with the onset of the pion-related γ -ray emission; (2) the decay constant of the time-extended neutron emission is slightly larger; and (3) different power-law neutron energy spectra were assumed during the impulsive and second phases. Assuming a power-law energy spectrum ($\alpha E_n^{-s_1}$) with $s_1 = 2.9 \pm 0.1$ in the impulsive phase and $4.1 < s_2 < 4.4$ in the second phase, we obtained the good fit ($\chi^2 = 2.6$) of the calculated increase to the Climax data shown in Figure 7. A high-energy cutoff of 2 GeV was assumed for both spectra. The total integrated neutron emissivity at the Sun extrapolated from the energy range relevant to NM observations to $E \geq 100$ MeV was $3.5 \times 10^{30} \text{sr}^{-1}$. When we take the decay of the prolonged high-energy γ -ray emission to be less than 1300 s, the calculated NM count rate increase is too small after 2100 UT and the reduced $\chi^2 \sim 8$. We believe that the fit of the calculated to the observed NM increase at Climax shown in Figure 7 is the best that can be achieved without increasing the number of free parameters.

4. ONSET TIME OF THE SOLAR PROTON INCREASE

We argue that the protons detected by NMs belong to a population different from the one responsible for the neutrons and γ -rays because the first interplanetary protons in the third phase originated several minutes after the onset of the γ -ray emission. Referring to Figure 1 it is evident that there were large station-to-station differences in the 5 minute NM count rate increases during the solar cosmic-ray event on 1990 May 24. At Climax and Mexico City the increase due to solar neutrons is clearly evident, as indicated by the darkened areas in Figure 1. The increase at Climax due to solar neutrons around 2050 UT was ~ 2 times larger than the subsequent increase due to solar protons. At Mexico City the ratio of the increases due to solar neutrons and solar protons was ~ 8 . Mount Wellington, on the nightside of the Earth, did not detect any solar neutrons and only recorded the increase due to solar protons. The onset time at Mount Wellington as deter-

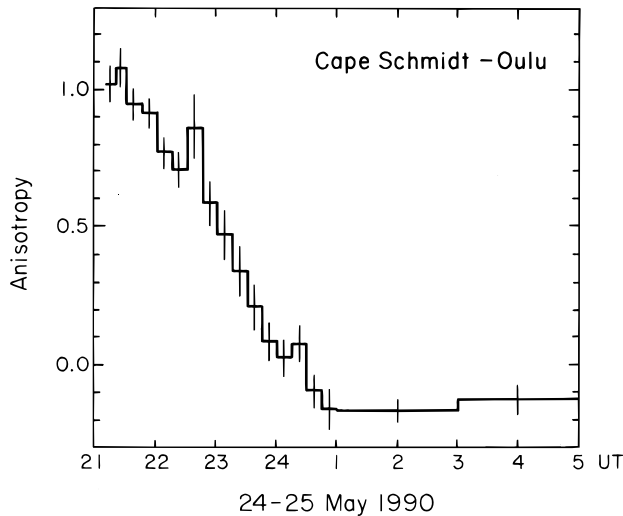


FIG. 8.—Anisotropy-time profile of the solar proton flux derived from the NM records at Cape Schmidt ($P_c = 0.43$ GV) and Oulu ($P_c = 0.82$ GV) for the second increase on 1990 May 24.

mined from the 1 minute count rates was $2102:30 \pm 00:30$ UT and the intensity maximum occurred at 2115 UT, followed by a rapid decay until ~ 2230 UT, when a much slower decay prevailed for another 6 hr. At Oulu the largest increase occurred late in the event (~ 0100 UT) when the solar proton flux had become isotropic.

The rapid onset at ~ 2102 UT recorded by the Mount Wellington NM suggests that the initial solar proton flux was highly anisotropic. We have selected two high-latitude neutron monitors that had asymptotic viewing directions as far apart as possible to determine the solar proton anisotropy: Cape Schmidt, viewing close to the apparent source direction, and Oulu, that looked in a direction $\sim 140^\circ$ from Cape Schmidt.

The deduced anisotropy of the solar protons from 2110 UT on 1990 May 24 to 0500 UT on May 25 is plotted in Figure 8. The anisotropy of the $E > 500$ MeV solar proton flux was greater than 90% from onset until 2200 UT, after which it decreased but remained at $\sim 50\%$ until 2300 UT. We are unable to interpret the anisotropy at lower proton energies measured by the *IMP 8* spacecraft because it was in the dusk magnetosheath. We can only infer from other solar flare events that the anisotropy probably extended down to ~ 50 MeV (Lockwood, Debrunner, & Flückiger 1990).

We determined the onset time of the proton event as a function of energy using the method of Lockwood et al. (1990). Two examples of the intensity-time profiles of the *IMP 8* solar particle fluxes during the second increase are shown in Figure 9. The proton fluxes for $E < 80$ MeV on the *IMP 8* cosmic-ray telescopes are obtained from measurements of energy loss versus total energy (dE/dx vs. E) derived from pulse height analysis of protons stopping in the scintillator array and for $E > 80$ MeV by the multiple dE/dx measurements of charged particles that penetrate the stacked array (McGuire & von Rosenvinge 1984; McGuire, von Rosenvinge, & McDonald 1986; Goswami et al. 1988). In Figure 9 we indicate the average background count rates before the increase. The errors shown are statistical only but this is the largest source of error for the 5 minute time resolution data. The onset time of a rate increase in any energy channel was determined by a linear fit of the logarithm of the intensity as a function of time before the maximum and extrapolating the straight line to the time of no count rate above background. The resulting onset times

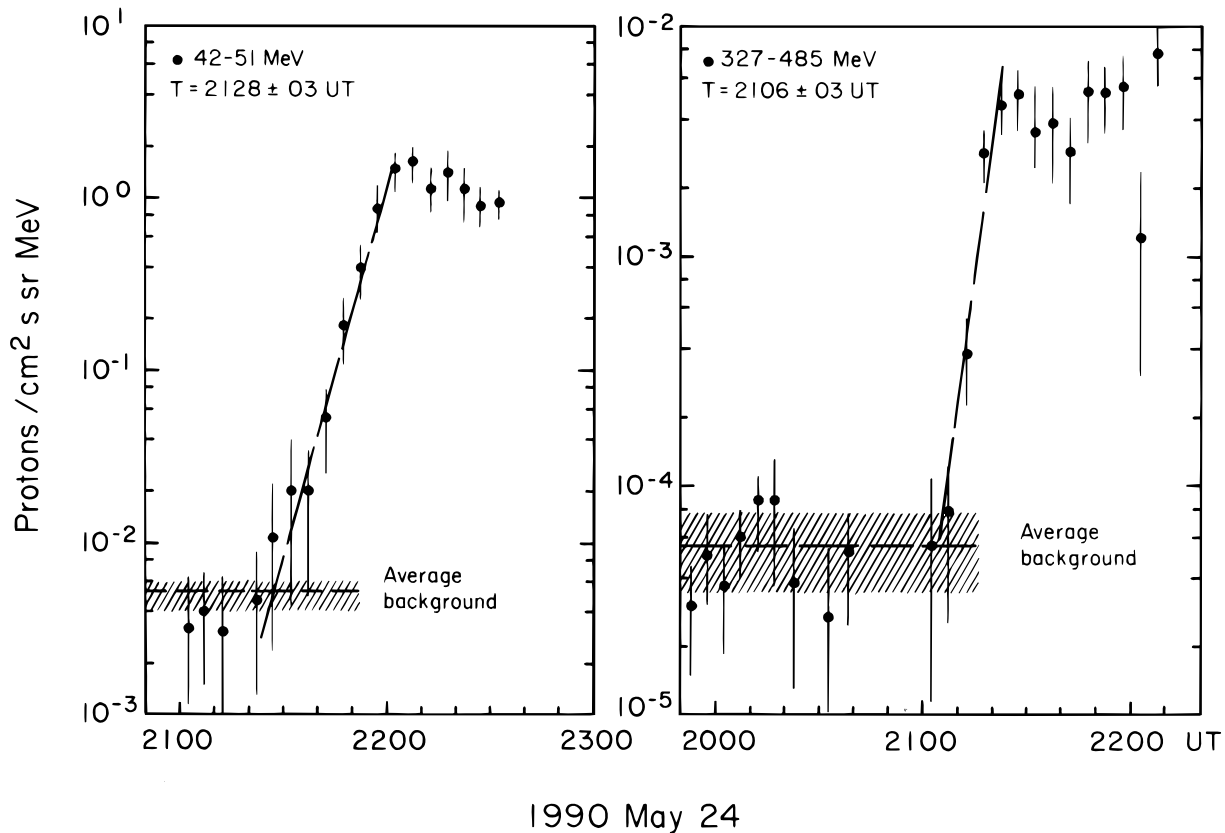


FIG. 9.—Intensity-time profiles of solar protons for median energies ~ 46 MeV and ~ 387 MeV on 1990 May 24 as observed by *IMP 8*

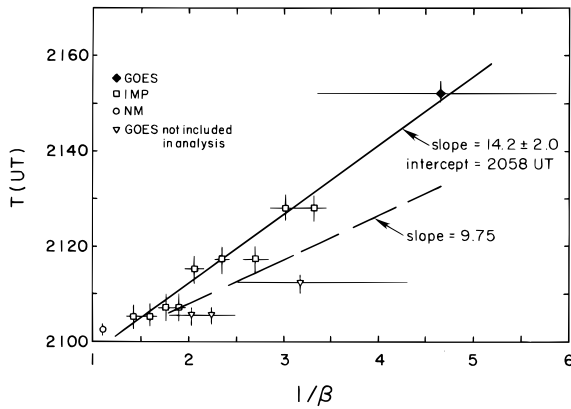


FIG. 10.—Onset time as a function of $1/\beta$ for the second increase on 1990 May 24, where β is the proton speed in units of the speed of light. The energy spread for each channel and the uncertainty in the determination of onset time are indicated. For details see the text.

for the different energy channels in the *IMP 8* detector are given in Table 2. We attempted to include the onset times for the differential energy channels of the *GOES* detector (Sauer 1993), but most of the lower energy channel data were contaminated by higher energy protons or electrons. Only the onset time for the 15–44 MeV channel is consistent with the times obtained from the *IMP 8* and NM data.

We use the onset times for the solar protons listed in Table 2 to support the premise that the solar protons were not injected into the interplanetary magnetic field until several minutes after the impulsive γ -ray burst at ~ 2048 UT and that the first relativistic solar protons producing the NM increases may have been delayed by 2 ± 1 minutes with respect to the lower energy ones. These onset times are plotted in Figure 10 as a function of $1/\beta$ where $\beta = v/c$ (Lockwood et al. 1990). The time of arrival of the first protons at the Earth, $T(E)$, with speed βc is

$$T(E) = T_0(E) + \{ \xi(E)/c \} \{ 1/\beta(E) \}, \quad (3)$$

where $T_0(E)$ is the time when the first protons were injected into the interplanetary magnetic field at the Sun. This value must be increased by 500 s in order to agree with the times of the γ -ray and neutron emissions. $\xi(E)$ is the distance traveled by the solar protons from the injection region to

TABLE 2

ONSET TIME FOR THE SOLAR PROTON INCREASE ON 1990 MAY 24

Median Energy MeV	Energy Range (MeV)	$1/\beta$	Onset Tim (UT)
<i>IMP 8:</i>			
46	42–51	3.31	2128 \pm 02
56	51–63	3.02	2128 \pm 02
71	63–81	2.71	2117 \pm 03
99	92–107	2.35	2117 \pm 03
135	121–154	2.06	2115 \pm -3
165	154–178	1.90	2107 \pm 03
200	178–229	1.76	2107 \pm 03
267	229–327	1.59	2105 \pm 03
387	327–485	1.41	2106 \pm 03
Neutron monitor	> 500 MeV	1.02	2102.5 \pm 0.5
<i>GOES:</i>			
138	110–500	2.04	2105 \pm 03 ^a
103	84–200	2.30	2105 \pm 03 ^a
50	39–82	3.18	2112 \pm 03 ^a
22	15–44	4.65	2152 \pm 03

^a Not used in the analysis of the onset times.

the observer at the Earth. If T_0 and ξ are constant, $T(E)$ is a linear function of $1/\beta$. For a most probable solar wind speed of 440 km s^{-1} (4 days AU^{-1}), the distance along the nominal interplanetary Archimedean spiral magnetic field line from the Sun to the Earth is $\sim 1.2 \text{ AU}$ and the slope of T as a function of $1/\beta$ is 9.75 minutes. However, we find that the slope of the best fit line to the data shown in Figure 10 is 14.2 ± 2.0 minutes corresponding to a path length of $1.7 \pm 0.3 \text{ AU}$.

Since the solar proton flux was highly anisotropic for about 1 hr after the onset of the event, there was no significant interplanetary diffusion taking place (Lockwood et al. 1990). Therefore, the fact that $\xi = 1.7 \text{ AU}$ implies that the solar protons traveled along interplanetary field lines that were much longer than the nominal spiral field lines. If the average solar wind speed had been as low as $\sim 185 \text{ km s}^{-1}$, an unlikely situation, then ξ could attain a value as large as 1.7 AU. However, from observations of coronal mass ejections (CME) on 1990 May 21 and 23 (Solar-Geophysical Data, Number 555, Part II, November 1990), there are indications of a distorted interplanetary magnetic field configuration. The estimated positions of these ejecta on 1990 May

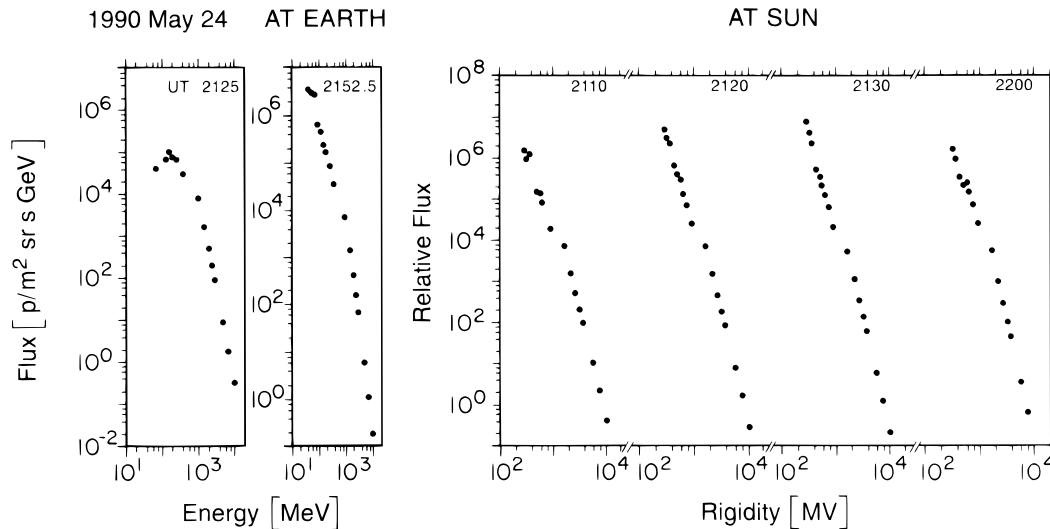


FIG. 11.—Solar proton fluxes at the Earth and the Sun during the anisotropic phase of the solar proton increase at the Earth on 1990 May 24. For details see the text.

24, assuming a propagation speed of $\sim 600 \text{ km s}^{-1}$, are at $\sim 0.6 \text{ AU}$ and $\sim 1 \text{ AU}$. We also found from the NM data that the apparent source direction of the solar protons was $\sim 40^\circ$ east of the Earth–Sun line rather than being $\sim 50^\circ$ west, as expected in highly anisotropic solar cosmic-ray events for a nominal interplanetary magnetic field (Lockwood et al. 1990; Debrunner et al. 1993). Furthermore, during the hour when the solar proton flux at the Earth was most anisotropic, the apparent source direction shifted $\sim 30^\circ$ in longitude and $\sim 45^\circ$ in latitude indicating a complex, rapidly evolving interplanetary magnetic field in the vicinity of the Earth (see also Morishita et al. 1995). We believe, therefore, that the interplanetary magnetic field configuration between the Sun and the Earth differed from the nominal Parker field, but with little turbulence.

There is evidence in Figure 10 that the first nonrelativistic protons were injected into the interplanetary magnetic field at the Sun at $2052 \pm 02 \text{ UT}$ and the first relativistic solar protons producing the second NM count rate increase may have been delayed by as much as 2 ± 1 minutes. This implies that the solar protons were not injected until 4–6 minutes after the impulsive γ -ray burst at 2048 UT.

5. ENERGY SPECTRA OF THE INTERPLANETARY SOLAR PROTONS

Since the solar proton flux at Earth after 2101 UT on 1990 May 24 was highly anisotropic for more than 1 hr, we can construct the energy spectrum (or rigidity spectrum) in interplanetary space near the Sun. We use the method described by Lockwood et al. (1990). We deduce the flux of solar protons with $E > 500 \text{ MeV}$ near the Earth by comparing the observed NM intensity increases with those calculated using the formula (Smart, Shea, & Tanskanen 1971):

$$\delta N_P(P_t) = \int_{P_c}^{\infty} \Phi_P(P, t) F(\theta, t) S_P(P) dP, \quad (4)$$

where δN_P is the response of a sea level NM, P_c is the vertical cutoff rigidity, Φ_P is the differential flux of solar protons as a function of rigidity P , F is the pitch angle distribution, and S_P is the specific yield function of a NM for protons. We assume the pitch angle distribution to be independent of energy above 500 MeV. For the solar proton flux less than 500 MeV we used the measurements of the *IMP 8* spacecraft averaged over $4\pi \text{ sr}$ (Debrunner et al. 1984).

We have plotted at the left in Figure 11 two samples of the differential solar proton energy spectrum at the Earth. These spectra were constructed using the *IMP* data from $\sim 15 \text{ MeV}$ to 500 MeV and the NM data above 500 MeV . Solar proton spectra at the Earth were also deduced for 16 other time intervals from the onset at 2102 UT on May 24 to 0400 UT on May 25. We see that the energy spectra near the Earth cannot be described by a simple exponential or power law in energy. A pronounced maximum at 200 MeV is observed during the earlier phase of the event, illustrated by the spectrum at 2125 UT. We attribute the turnover of the spectrum at lower energies at 2125 UT to velocity dispersion. At 2152:30 UT little dispersion is evident. The agreement at $\sim 500 \text{ MeV}$ between the spectra deduced from the NM and the *IMP 8* measurements is within a factor of ~ 3 . This is good agreement considering that *IMP 8* was not in the interplanetary magnetic field.

We also show in Figure 11 the relative solar proton flux at the Sun as a function of rigidity. The spectra at the Sun were constructed by using the solar proton fluxes at the Earth for the period of large anisotropy and assuming a path length of 1.7 AU for the protons between the Sun and the Earth (Lockwood et al. 1990). It was only possible to construct the spectra at the Sun for the time interval 2110–2200 UT because of the limited amount of data from *IMP 8*. The solar proton flux, dJ/dE , is plotted as a function of rigidity for comparisons with diffusive shock acceleration models. The discontinuity in the fluxes at $\sim 500 \text{ MeV}$ deduced from the NM and *IMP 8* data is more evident in these spectra.

Lockwood et al. (1990) found that the solar proton fluxes, dJ/dE , on 1978 May 7 and 1984 February 16 at the Sun as a function of rigidity are best described by a power law in rigidity, suggesting diffusive coronal shock acceleration. The spectral indices of $dJ/dE \propto P^{-\gamma}$ for the 1990 May 24 solar proton increase are listed in Table 3. Assuming diffusive coronal shock acceleration, the shock compression ratio is $r = (\gamma + 2)/(\gamma - 1)$. We find that the shock compression ratios listed in Table 3 are about the same as those of the 1978 and 1984 solar cosmic-ray events and suggest a weakening of the shock between 2110 UT and 2200 UT. These ratios are in agreement with the model of Ellison & Ramaty (1985).

The intensity of the injected solar protons with $E > 30 \text{ MeV}$ is estimated to be $\sim 9 \times 10^{28}$ protons/(sr s) and it remained constant to within a factor 4 from 2110 to 2200 UT. Assuming that the protons at the Sun were emitted into interplanetary space over a solid angle of 2 sr , the total number of protons above 30 MeV during the time interval 2105:00–2207:30 UT was 7×10^{32} . This is about 10 times smaller than that previously estimated by Debrunner et al. (1993). At that time the *IMP 8* data were not available so that the hardening of the spectra at low energies, evident from the second panel of Figure 11, was not considered.

6. DISCUSSION

6.1. Observational Results

Since a NM is an integral detector (measuring neutrons above some threshold energy), the count rate increase provides little information about the neutron energy spectrum unless a neutron production time profile at the Sun is available. The difference between the intensity-time profile of the neutron emission at the Sun and of the NM increase then depends on the solar neutron energy spectrum because of the energy-dependent transit time of the neutrons from the Sun to the Earth. Thus, the difference between the sharp onset of the Climax NM count rate increase at 2049 UT and

TABLE 3
PARAMETERS OF THE ENERGY SPECTRUM AT THE SUN FOR THE PROTONS
PRODUCED IN THE THIRD PHASE OF THE 1990 MAY 24 SOLAR
FLARE EVENT

Time at the Sun (UT)	Spectral Index γ^a	Correlation Coefficient R^2	Compression Ratio of the Shock, r
2110	4.0	0.98	2.0
2120	4.4	1.00	1.9
2130	4.6	1.00	1.8
2145	4.6	1.00	1.8
2200	4.6	0.98	1.8

^a Where γ is defined by: $dJ/dE = AP^{-\gamma}$.

the onset of the γ -ray emission indicates a sharp upper energy cutoff at ~ 2 GeV in the neutron production—more rapid than an exponential roll-off. An exponential roll-off superposed on a power-law neutron energy spectrum of the form $\exp(-E/E_0)$ that extends out to \sim GeV does not fit the data. The exponential roll-off is not fast enough. This upper energy threshold is an important key to determining the shape of the high-energy proton spectrum that produced the neutrons.

From the simulations of the excess count rate of the Climax NM during the first increase, we find that the shape of the neutron emissivity spectrum was different during the impulsive and second phases. This is consistent with a high-energy (> 200 MeV) proton spectrum that softens after the second peak in the impulsive phase. The different decay times of the γ -ray line emissions and 60–95 MeV γ -rays in Figures 2 and 6 indicate a hardening of the neutron spectrum throughout the second phase. Such a hardening of the neutron spectrum during the second phase, which we did not consider in our analysis, would bring the calculated and observed count rate increases into still better agreement.

We now compare the number of solar protons released at the Sun into interplanetary space during the third phase with the number of solar protons required for the observed 2.2 MeV γ -ray line fluence and the neutron production during the first and second phases. The total number of protons escaping from the Sun with $E > 30$ MeV during the interplanetary solar proton increase from 2105:00 to 2207:30 UT is estimated to be 7×10^{32} . To estimate the number of solar protons with $E > 30$ MeV producing the γ -ray and neutron emissions, we use the results of Hua & Lingenfelter (1987) where the solar protons have an isotropic pitch angle distribution and an energy spectrum described by a power law with a spectral index of 2.5–3.0. We then find that the observed 2.2 MeV γ -ray line fluence of ~ 1000 photon cm^{-2} requires 5×10^{33} to 1×10^{34} protons with $E > 30$ MeV. Similarly, the neutron fluence of 3.5×10^{30} neutrons sr^{-1} with $E > 100$ MeV deduced from the fit of the calculated to the observed NM count rate increase at Climax also corresponds to $\sim 10^{34}$ protons greater than 30 MeV. Hence the number of solar protons producing the second NM count rate increase was only 7%–14% of the number of protons required to generate the solar neutrons as observed in the first increase. Ramaty et al. (1993) have compared the numbers of interacting and

interplanetary protons for 10 solar flare events between 1972 and 1982 and found highly variable ratios. These ratios depended on the assumed elemental composition of the ambient gas and accelerated particles. For only two events, 1982 June 3 and 1980 June 21, were solar neutrons as well as γ -rays and interplanetary protons detected. In these two events the ratio of interacting to escaping protons was in the range of 0.77–4 for 1982 June 3 and 3–17 for 1980 June 21. These values compare reasonably well to that for the 1990 May 24 solar flare event. The question now is: are the interplanetary particles simply protons that leaked out from the regions where the γ -rays neutrons were produced or were they freshly accelerated remotely at a later time by a coronal shock? The data suggest that the interplanetary protons were not from the population of energetic particles that produced the neutron and γ -ray emissions but were freshly accelerated.

6.2. Comparison with the Results of Kocharov et al. (1994)

Kocharov et al. (1994) concluded from measurements of the H α line, γ -ray, and microwave emissions that the neutron increase observed by the Climax NM was produced by two neutron injections. They “attribute the whole event as due to a prompt acceleration of both electrons and protons by the shock and subsequent deceleration of the trapped particles while they propagate inside the magnetic loops.” This is similar to the approach here in that we assume two phases for the neutron injection.

First, we find that the intensity-time profile of their two-component neutron injection function ($E > 100$ MeV) approximately tracks the pion-related γ -ray emission. From the comparison of the two neutron production-time profiles shown in Figure 12a we see that the main difference lies in the faster decay time (~ 260 s) for the second phase of the neutron production used by Kocharov et al. (1994). They assumed that the decay rate was the same as that of the 2.2 MeV γ -ray flux reported by Terekhov et al. (1993). They also assumed that after 2052 UT the majority of the counts in the 60–95 MeV γ -ray energy band of the PHEBUS detector was due to solar neutrons. As we show in Appendix A, it does not appear that the bulk of the counts in the highest energy channel of the PHEBUS detector was due to neutrons but rather was due to pion-related γ -rays that were still present at the end of the measurements at 2058 UT. Furthermore, the Climax NM was apparently still

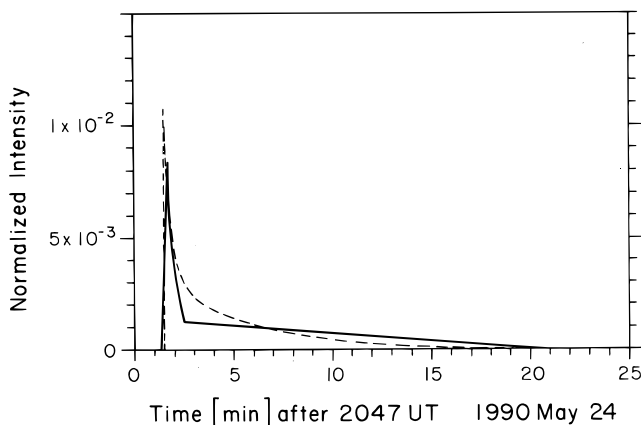


FIG. 12a

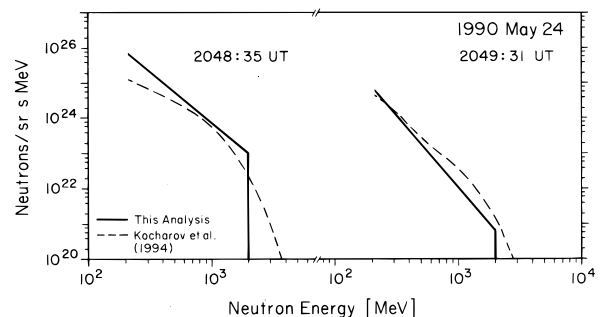


FIG. 12b

FIG. 12.—(a) Comparison of the neutron injection-time profile of this paper (solid line) and that of Kocharov et al. (1994) (dotted line). (b) Comparison of the neutron energy spectrum of this analysis and that of Kocharov et al. (1994) at two different times.

responding to solar neutrons after 2103 UT. From the Mexico City NM data and the asymptotic viewing directions of that station, we conclude that there were no solar protons observed earlier than 2110 UT. This extends the duration of the neutron emission to ~ 20 minutes in contrast to the shorter neutron production time assumed by Kocharov et al. (1994). In a recent paper Kovaltsov et al. (1995) combined the NM data of Climax and Mexico City and found that a decay time for the neutron production of greater than 260 s fits the data better.

Second, the neutron emissivity spectra for greater than 200 MeV deduced by Kocharov et al. (1994) and plotted in Figure 12*b* are similar to those calculated here using only three parameters.

6.3. Relationship of the Decay of the 4–7 MeV, 2.2 MeV, and Pion-Related γ -Rays to the Neutron Production Time

In the 1990 May 24 solar flare event we have found that if we take the time-extended neutron emission to track the intensity-time profile of the pion-related γ -rays, we can obtain a reasonable fit to the observed count rate increases at the Climax and Mexico City NMs. On the other hand, the decay constant of ~ 240 s for the 2.2 and 4–7 MeV γ -ray emissions in the second phase of the neutron emission shown in Figure 6 is too short to describe the NM increases that lasted until 2115 UT.

We believe that the pion-related γ -ray emission is a better indicator of high-energy neutron production than the 2.2 MeV line emission. For the 1982 June 3 solar flares, Dunphy & Chupp (1994) found that the decay of the greater than 25 MeV events measured by GRS/SMM, the count rate of which was primarily due to pion-related γ -rays, could be fitted by a two-step decay with time constants of 69 ± 8.5 and 700 ± 180 s. These results suggest that the neutron production lasted for ~ 20 minutes (Chupp et al. 1987). In an earlier analysis the intensity-time profile of the 2.2 MeV line of the 1982 June 3 event was taken to represent the time dependence of the low-energy neutron production (Prince et al. 1983). It was found that the decay constants (using a single exponential decay) for the 2.2 MeV γ -ray line and the 4–7 MeV γ -ray band emissions were ~ 160 s and 70 s, respectively. This decay is too fast to produce the neutron count rate increases measured by the SMM detector and the Jungfraujoch NM on 1982 June 3 (Chupp et al. 1987). The long duration of the high-energy neutron production can be associated with the transport and acceleration of protons trapped in turbulent coronal loops that probably evolved in time (Trottet et al. 1994).

These measurements of long decay times for high-energy γ -rays associated with the production of high-energy neutrons preclude an impulsive solar neutron emission. For example, in the 1990 May 24 solar neutron increase the high-energy neutron production during the second phase was twice that in the impulsive phase. It is also evident that the decay of the high-energy neutron emission at the Sun is much slower than the decay of the 2.2 MeV and the 4–7 MeV γ -ray line emission, requiring an evolving proton spectrum at the Sun during the second phase.

6.4. Production of the Neutrons and Acceleration of the Protons at the Sun

The present measurements of the 1990 May 24 event show that the γ -ray spectrum, and hence the spectrum of interacting ions, was highly variable during the event—

changing between the first and second peak of the impulsive phase and between the impulsive and second phase. Previous multiwavelength studies of γ -ray and neutron events have shown that such changes of the γ -ray spectrum generally correspond to particle acceleration in spatially separate regions (Chupp et al. 1993; Trottet et al. 1994; Trottet 1994). For the 1990 May 24 event it is not possible to tell from the data if the two impulsive peaks arise from two different regions. Nevertheless, H α and microwave observations reported by Kocharov et al. (1994) suggest that the acceleration of the flare protons in the impulsive and second phase occurred in two different loops or regions. This was shown to be the case for the 1982 June 3 event (Trottet et al. 1994) which in many aspects is similar to the 1990 May 24 event.

The long duration phase on 1990 May 24 may be explained as in other events by continuous acceleration, such as proposed by Akimov et al. (1991) for the 1991 June 15 flare and by Mandzhavidze & Ramaty (1993) for the 1991 June 11 flare or by transport and acceleration in turbulent magnetic loops (Ryan & Lee 1991). However, these models do not address the presence of high-energy solar protons in interplanetary space after a solar flare. Indeed, Ryan & Lee assumed that the flare loop is taken to be closed with no loss of particles into interplanetary space. The present observations of the 1990 May 24 event strongly suggest that the interplanetary protons do not belong to the populations of protons that produced the γ -rays and neutrons. The delay time (4–6 minutes) of the onset of the greater than 500 MeV solar proton injection into interplanetary space with respect to that of the γ -ray and neutron emissions and the long duration of several hours for the interplanetary solar proton event strongly argue against direct leakage out from the flaring region. Furthermore, the energy spectrum of the interplanetary solar protons extended beyond 4 GeV. That is inconsistent with the neutron energy upper limit (2 GeV) deduced from the Climax NM data.

Kocharov et al. (1994) reported observations of a Moreton wave in the 1990 May 24 event, which is estimated to have started between 2047:40 and 2047:50 UT in coincidence with the onset of the γ -ray emission. They estimated that the shock speed was 1600 km s^{-1} . If we ascribe to the Moreton wave a coronal shock of the same speed, the shock moved about 0.85 solar radii in the time interval of 380 s between the start of the Moreton wave and the time at which the first relativistic solar protons were injected into the interplanetary magnetic field. It seems unlikely that these greater than 500 MeV solar protons could have been accelerated between 2047:50 and 2049:24 UT in the impulsive phase of the solar cosmic-ray event and then stored at the Sun for about 5 minutes until 2054 UT when they were released into interplanetary space. In such a scenario it would seem most unlikely that the first solar particles to leak out would be the lower energy ones. The onset times of the solar proton event plotted in Figure 10 clearly indicate that the lower energy protons were accelerated earlier or leaked out first. A possible scenario is that the protons observed at Earth starting at 2102:30 UT were “freshly” accelerated at the Sun as the shock moved outward from the Sun into regions of open field lines (Murphy et al. (1987). An alternative explanation would be an energy release in open magnetic structures at a remote site from the flaring region leading to acceleration by a shock or some other

process. Such an energy release could have been triggered by the Moreton wave as it moved away from the flaring site. In either case, the interplanetary protons are not directly related to the protons producing the solar γ -rays and neutrons. This implies that the acceleration of the first interplanetary protons took place while other protons at the Sun were producing solar γ -rays and neutrons for ~ 20 minutes.

7. CONCLUSIONS

The 1990 May 24 solar cosmic-ray event can be naturally divided into three phases of particle acceleration observed at Earth by spacecraft and NMs. The PHEBUS detectors on the *Granat* spacecraft measured γ -rays up to 95 MeV during the impulsive phase (2047:50 to 2049:24 UT), which had two peaks, and during the second phase (starting at 2049:24 UT). High-energy neutrons arising from both of these phases were detected by NMs on the daylight side of the Earth. NMs and solar particle detectors on the *IMP 8* and *GOES* spacecraft responded to solar protons in the third phase starting at 2052 UT and lasting until at least 2200 UT. We conclude the following.

1. The γ -ray spectrum was highly variable during the event, changing between the first and second peak in the impulsive phase and between the impulsive and second phase. The emission of pion-related γ -rays started after the first peak of the impulsive phase.

2. The integrated neutron emission at the Sun during the first increase observed by NMs on 1990 May 24 was one of the largest ever measured and was $3.5 \times 10^{30} \text{ sr}^{-1}$ for $E > 100 \text{ MeV}$.

3. The neutron energy spectra during the first and second phases are described by power laws with spectral indices of 2.9 ± 0.1 from 2048:18 to 2049:24 UT (the latter part of the impulsive phase) and 4.25 ± 0.15 after 2049:24 UT. This two-component energy spectrum gives a reasonable fit to the count rate increase at the Climax NM. The softening of the neutron energy spectrum between the impulsive and second phases is consistent with the γ -ray measurements indicating also a softening of the spectrum of the interacting protons in this time period (see Figs. 2a and 6).

4. The high-energy neutron production time profile tracked that of the pion-related γ -rays and was of prolonged duration (~ 20 minutes). The slow decay of the neutron production is in contrast to the much faster decay of the 2.2 and 4–7 MeV γ -ray line emissions.

5. The NM increase that started at 2102:30 UT on 1990 May 24 had a peak solar proton flux at the Earth of $1.0 \times 10^5 P^{-(5.3 \pm 0.2)} (\text{m}^2 \text{ sr s GV})^{-1}$. It was similar in shape to that measured in other solar cosmic-ray events (Lockwood et al. 1990) and was anisotropic for more than 1 hr after the onset, again similar to other solar cosmic-ray events (Lockwood et al. 1990). The maximum intensity for $P > 1.5 \text{ GV}$ was $4.5 \times 10^3 (\text{m}^2 \text{ sr s})^{-1}$.

6. We estimate that the number of escaping protons with $E > 30 \text{ MeV}$ associated with the second NM increase was only 7%–14% of the number of protons required to produce the observed γ -ray and neutron emissions.

7. The delay time of the onset of the solar proton injection into interplanetary space with respect to that of the γ -ray and neutron emissions and the fact that the upper energy limit of the neutrons is smaller than that of the interplanetary protons strongly suggest that the interplanetary protons were “freshly” accelerated at the Sun after 2052 UT and were not directly related to the interacting protons producing the γ -rays and neutrons. This acceleration of interplanetary protons started 4–6 minutes after the first neutrons were produced and about 15 minutes before the high-energy neutrons ceased being produced at the Sun.

We thank M. A. Shea and L. Gentile for maintaining the GLE database and the numerous PIs for providing their NM data. We especially appreciate R. Pyle and T. Mathews for sending us the data from the NMs at Climax and Calgary, respectively. One of the authors (H. D.) thanks the University of New Hampshire Space Science Center for the support and hospitality during his visit there. This research was supported in part by the US National Science Foundation (ATM 91-23815), the Swiss Science Foundation (NF 20-31130.91), and the French Centre National d'Etudes Spatiales (contracts 94-0208 and 94-0333).

APPENDIX A

DETERMINATION OF THE NEUTRON CONTAMINATION IN THE GREATER THAN 60 MeV CHANNELS OF THE PHEBUS DETECTOR AFTER 2050 UT

In order to deduce the intensity and decay rate of the pion production after the impulsive phase, we assumed that after 2052 UT the count rates in the high-energy PHEBUS channel (60–95 MeV) were mainly due to γ -rays. We first estimate the effect of solar neutrons on the greater than 75 MeV PHEBUS count rates by calculating the greater than 75 MeV solar neutron flux (neutrons $\text{cm}^{-2} \text{ s}$) at the Earth as a function of time using the intensity-time profile of neutron production in Figure 5 and the value of $Q(E_n)$ in equation (2) that gives a best fit of the calculated to the observed count rate increase at Climax shown in Figure 7. We show in Figure 13 the neutron intensity at the earth for $E > 500 \text{ MeV}$ and $75 < E < 500 \text{ MeV}$ as a function of time from 2047 to 2115 UT. First, we find that there is indeed a bump in the greater than 500 MeV neutron flux from 2049:30 to 2051:30 UT due to neutron production during the impulsive phase. In contrast, the $75 < E < 500 \text{ MeV}$ neutron flux is zero at 2050 UT. Then it increases by a factor of 3 from 2052 to 2057 UT, the end of the data file from PHEBUS. Such an increase in the greater than 75 MeV count rate of PHEBUS is not observed. We therefore conclude that the greater than 75 MeV count rate of PHEBUS after 2052 UT was primarily due to pion-related γ -rays.

We estimate that the maximum excess count rate of the bump in the 75–95 MeV range due to neutrons with $E > 500 \text{ MeV}$ was $1.7 \text{ counts s}^{-1}$ compared with an observed excess rate from 2050:00 to 2050:47 UT of $1.7 \pm 0.8 \text{ counts s}^{-1}$ above $3.6 \pm 0.4 \text{ counts s}^{-1}$ from 2049:36 to 2050:00 UT. We see from Figure 13 that the maximum flux greater than 500 MeV solar neutrons in the bump is $\sim 1 \text{ neutron cm}^{-2} \text{ s}^{-1}$. The average path length for a neutron incident perpendicular to the axis of the PHEBUS detector is $\sim 43 \text{ g cm}^{-2}$. From the estimated mean free path of 140 g cm^{-2} for a neutron above 500 MeV in the

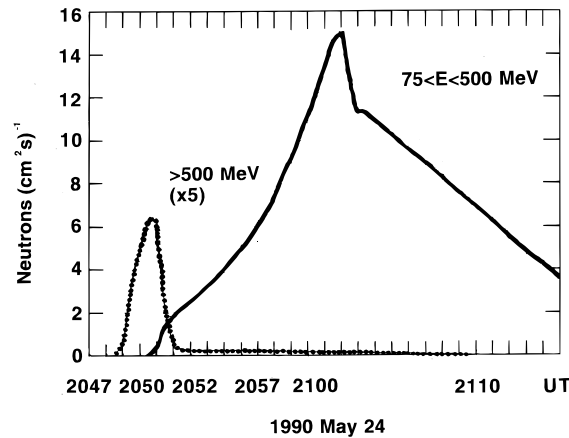


FIG. 13.—Neutron intensity ($\text{cm}^{-2} \text{s}^{-1}$) at the Earth as a function of time for the energy ranges $75 < E < 500 \text{ MeV}$ and $E > 500 \text{ MeV}$ on 1990 May 24. The greater than 500 MeV curve has been multiplied by a factor of 5.

BGO scintillator, we find that the neutron interaction probability is $\sim 25\%$, much smaller than the figure used by Terekhov et al. (1993). Taking the geometrical area of a PHEBUS detector as 100 cm^2 , the probability for the reactions $n + p \Rightarrow n + p + \pi^0$, $n + n \Rightarrow n + n + \pi^0$, $\pi^0 \Rightarrow 2\gamma$ as 0.35 and the probability that the γ -ray lies in the energy range 75–95 MeV as 0.1, we find that the excess count rate of the bump was $1.7 \text{ counts s}^{-1}$ corresponding to a detection efficiency of 1%–2% for greater than 500 MeV neutrons.

In a second estimate of the contamination of the 75–95 MeV channel from solar neutrons, we first assume that all the counts in this energy window after 2053 UT were due to neutrons. We then estimate the contributions to the count rate in the lower energy channels due to solar neutrons by assuming that the PHEBUS detector efficiency for energetic neutron detection is not a strong function of neutron energy. In Table 4 we list the ratio of the average differential count rate in the 75–95 MeV channel (in $\text{counts s}^{-1} \text{ MeV}$) to those in other channels during the time interval 2053 to 2057:40 UT. From Table 4 we see that after 2053 UT the neutron contributions to the count rate were $\sim 65\%$, $\sim 50\%$, and 10% – 20% in channels 60–75 MeV, 37–60 MeV, and 8.75–26 MeV, respectively. (In all channels the statistical uncertainty in the 8 s average count rates in this time interval is $\sim 15\%$ – 20%). After we had subtracted the assumed solar neutron contribution in the 75–95 MeV channel from the count rate ($\text{MeV}^{-1} \text{ s}^{-1}$) in each channel, we determined the exponential decay constant of these channels below 75 MeV. An example of one of these decay curves is shown in Figure 14. Table 4 shows the decay constant as a function of γ -ray energy for $E < 95 \text{ MeV}$. In Figure 15 we have plotted the decay constant τ as a function of the mean energy of the channel. The decrease of the decay constant with decreasing energy at $E < 30 \text{ MeV}$ may be due to electron bremsstrahlung production and/or hardening of the proton energy spectrum. Assuming that τ is independent of energy for $E > 30 \text{ MeV}$, we find $\tau = (9.0 \pm 1.1 \times 10^2 \text{ s})$ for the γ -ray flux in the 75–95 MeV channel indicative of the pion production shown in Figure 5. It appears that the upper limit of the count rate in the 75–95 MeV energy window due to direct neutrons after 2053:40 UT is $\sim 30\%$. This implies that more than 70% of the count rate was due to γ -rays. The decay constant deduced by this method represents a lower limit to the decay constant of the pion production.

APPENDIX B

SENSITIVITY OF NEUTRON MONITORS TO SOLAR NEUTRONS

In the model of nucleon-nucleus interactions used by Debrunner et al. (1983, 1989, 1990) to calculate the response functions of NMs, only the intranuclear cascade is considered and the simulations of the nucleonic cascades in the atmosphere are based on the total cross section of the nucleon-nitrogen interactions and the detailed p - p and p - n cross sections for elastic and inelastic scattering. This approach should be correct above 200 MeV where the de Broglie wave length of the incident nucleon is small compared with the size of the nucleus. Shibata (1994) uses detailed neutron-nucleus cross sections and assumes a $\sim 30\%$ contribution from elastic neutron-nucleus collisions to the total interaction probability at $E > 200 \text{ MeV}$. The calcu-

TABLE 4
GAMMA-RAY DECAY RATES OF $-Y$ PHEBUS DETECTOR FROM 2052:58.5 TO 2057:40.5 ON 1990 MAY 24

Channel Number	Energy Range (MeV)	Average counts (MeV s^{-1})	Channel 40/Channel number	Standard Deviation Ratio	Decay Constant ^a (s)
40	75–95	0.171	968
39	60–75	0.275	0.622	0.279	732
38	37–60	0.345	0.496	0.093	982
37	26–37	0.588	0.291	0.048	929
36	19.2–26	0.848	0.202	0.050	564
34 and 35	12.25–19.2	1.156	0.148	0.033	559
32 and 33	8.75–12.25	1.938	0.088	0.036	458

^a Decay constant: $N(t) = N_0(1 - t/\tau)$, where τ is the decay time.

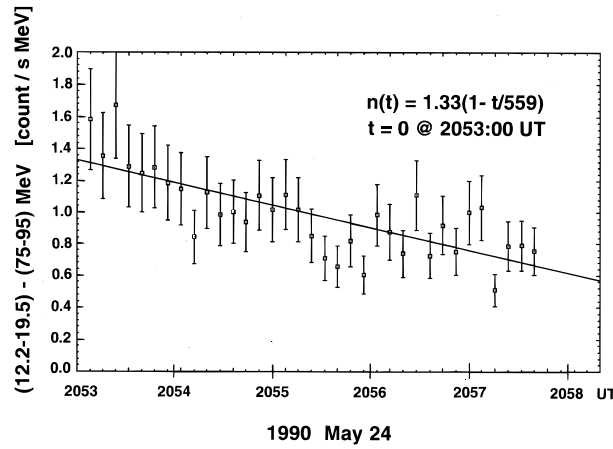


FIG. 14.—Intensity-time profile for the differential count rate of the PHEBUS γ -ray channel 12.2–19.2 MeV minus the count rate of the 75–95 MeV channel after 2053 UT in counts $(\text{s MeV})^{-1}$ during the 1990 May 24 solar event. For details see the text.

lations of Debrunner et al. have been revised since the analysis of 1982 June 3 solar neutron event (Debrunner et al. 1983; Chupp et al. 1987). At this time the Jungfrauoch IGY NM (with 18 counting tubes) was at an atmospheric depth of $h = 675 \text{ g cm}^{-2}$ and the angle to the subsolar point was $\theta = 25^\circ$ so that the air mass along the line of sight from the NM to the Sun was $L = 745 \text{ g cm}^{-2}$. During the 1990 May 24 event Climax was located at $h = 680 \text{ g cm}^{-2}$ and $\theta = 28.8^\circ$ so that $L = 776 \text{ g cm}^{-2}$ or within 5% of the atmospheric path length of Jungfrauoch for the 1982 June 3 event. The revisions made here were based on new comparisons of the response of an IGY NM to greater than 1000 MeV solar protons calculated by the method of Debrunner, Flückiger, & Lockwood (1982) and that deduced by Lockwood & Webber (1967) and Lockwood, Webber, & Hsieh (1974) from neutron monitor latitude curves. From 1 GeV to 9 GeV these proton response functions agree to within 20%. Therefore, we believe that the basic method of the Monte Carlo simulations by Debrunner and colleagues is correct at higher energies.

Shibata (1994) calculated the transport of solar neutrons through the Earth's atmosphere using a nuclear model in which elastic scattering of a neutron with an air nucleus is significant. In contrast to the simulations of Debrunner et al. (1983, 1989), the Shibata model predicts a sensitivity to solar neutrons with energies as small as 50 MeV. However, the contribution of neutrons with energies $50 < E < 200 \text{ MeV}$ to the count rate of an IGY NM is uncertain, and is probably small since the attenuation in the IGY NM shielding for neutrons is 20% at 200 MeV and increasing to 50% at 50 MeV (Hatton 1971).

For the 1990 May 24 solar flare event we have plotted in Figure 16 the neutron response S_n for the 12 tube IGY NM at Climax according to the original calculations by Debrunner et al. (1983). We have also plotted the revised response and S_n deduced by Shibata (1994). The error bar at 750 MeV ($\sim 30\%$) on the revised neutron response curve shown in Figure 16 is the best estimate of the uncertainty arising from the normalization process and suggests that the neutron response functions

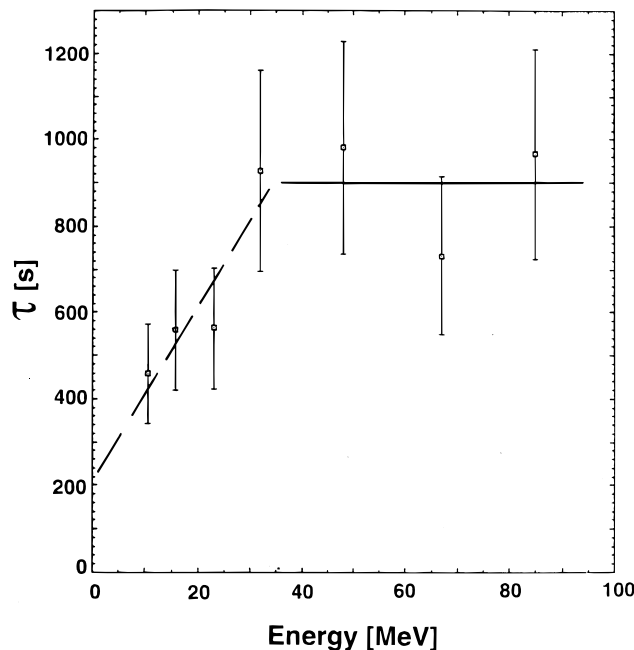


FIG. 15.—Decay constants of the 8.8–95 MeV γ -rays as a function of energy for the second phase of the 1990 May 24 event. Details are given in the text.

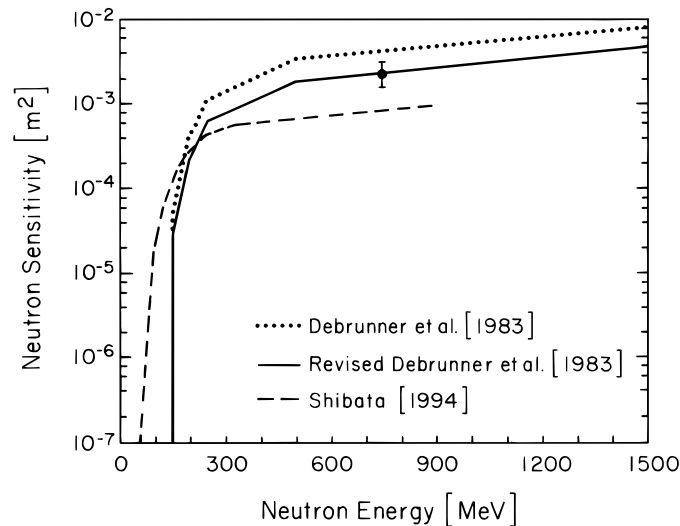


FIG. 16.—Comparison of the solar neutron responses (m^2) of a 12 tube IGY neutron monitor at Climax on 1990 May 24 as function of incident neutron energy at the top of the atmosphere for a slant depth of 776 g cm^{-2} derived originally by Debrunner et al. (1983) and then revised in the present analysis and that by Shibata (1994). For details refer to the text.

calculated by Shibata and Debrunner et al. may be within a factor of 2 above 200 MeV. However, below 200 MeV they diverge. Above 200 MeV some of the divergence may be explained by the fact that Shibata computed the sensitivity for the case of normal incidence which is not the case for the 1990 May 24 event (Debrunner et al. 1990, 1993). If the lateral spread of the nucleonic cascades is taken into account properly, S_n as calculated by Shibata (1994) will increase and the difference in the two response functions at above 200 MeV will decrease.

REFERENCES

- Akimov, V. V., et al. 1991, Proc. 22nd Internat. Cosmic-Ray Conf. (Dublin) 3, 73
- Barat, C., et al. 1988, in AIP Conf. Proc. 170, Nuclear Spectroscopy of Astrophysical Sources, ed. G. H. Share & N. Gehrels (New York: AIP), 95
- Chupp, E. L., et al. 1987, ApJ, 318, 913
- Chupp, E. L., et al. 1993, A&A, 275, 602
- Debrunner, H., Flückiger, E., & Lockwood, J. A. 1982, 8th European Cosmic-Ray Symp., (Rome), unpublished
- Debrunner, H., et al. 1983, Proc. 18th Internat. Cosmic-Ray Conf. (Bangalore), 4, 75
- Debrunner, H. et al. 1984, J. Geophys. Res., 89, 769
- Debrunner, H., Flückiger, E. O., & Stein, P. 1989, Nuclear Instr. Meth., A278, 573
- . 1990, Proc. 21st Internat. Cosmic-Ray Conf. (Adelaide), 5, 129
- Debrunner, H., Lockwood, J. A., & Ryan, J. M. 1993, ApJ, 409, 822
- Dunphy, P. P., & Chupp, E. L. 1994, in AIP Conf. Proc. 294, High Energy Solar Phenomena—a New Era of Spacecraft Measurements, ed. J. M. Ryan & W. T. Vestrand (New York: AIP), 112
- Ellison, D. C., & Ramaty, R. 1985, ApJ, 298, 400
- Goswami, J. N., et al. 1988, J. Geophys. Res., 93, 7195
- Hatton, C. J. 1971, in Prog. in Elementary Particles and Cosmic-Ray Physics, ed. J. G. Wilson & S. A. Wouthuysen, 10, 3
- Hua, X. M., & Lingenfelter, R. E. 1987, Solar Phys., 107, 351
- Kocharov, L. G., et al. 1994, Solar Phys., 155, 149
- Kovaltsov, G. A., et al. 1995, Proc. 24th Internat. Cosmic-Ray Conf. (Rome), 3, 155
- Lingenfelter, R. E., & Ramaty, R. 1967, in High-Energy Nuclear Reactions in Astrophysics, ed. B. S. P. Shen (New York: Benjamin), 99
- Lockwood, J. A., Debrunner, H., & Flückiger, E. O. 1990, J. Geophys. Res. 95, 4187
- Lockwood, J. A., & Webber, W. R. 1967, J. Geophys. Res., 72, 3395
- Lockwood, J. A., Webber, W. R., & Hsieh, L. 1974, J. Geophys. Res., 79, 4149
- Mandzhavidze, N., & Ramaty, R. 1993, Nucl. Phys. B, 13, 141
- McGuire, R. E., & von Roseninge, T. T. 1984, Adv. Space Res., 4, 117
- McGuire, R. E., von Roseninge, T. T., & McDonald, F. B. 1986, ApJ, 301, 938
- Morishita, I., et al. 1995, Proc. 24th Internat. Cosmic-Ray Conf. (Rome), 3, 220
- Murphy, R. J., et al., 1987, ApJ, 63, 721
- Prince, T. A., et al. 1983, in Proc. 18th Internat. Cosmic-Ray Conf. (Bangalore), 3, 79
- Pyle, R. 1991, private communication
- Ramaty, R., et al. 1993, Adv. Space Res., 13, 275
- Ryan, J. M., & Lee, M. A. 1991, ApJ, 368, 316
- Sauer, H. H. 1993, private communication
- Shea, M. A., Smart, D. F., & Pyle, K. R. 1991, Geophys. Res. Lett., 18, 1655
- Shibata, S. 1994, J. Geophys. Res., 99, 6651
- Smart, D. F., Shea, M. A., & Tanskanen, P. J. 1971, in Proc. 12th Internat. Cosmic-Ray Conf. (Hobart), 2, 483
- Talon, R., et al. 1993, Solar Phys., 147, 137
- Terekhov, O. V., et al. 1993, Astron. Lett., 19, 65
- Trottet, G. 1994, Space Sci. Rev., 68, 149
- Trottet, G., et al. 1994, A&A, 288, 647